



Exploring compact stellar structures in Finsler–Randers geometry with the Barthel connection

J. Praveen^a, S. K. Narasimhamurthy^b, B. R. Yashwanth^c

Department of P.G. Studies and Research in Mathematics, Kuvempu University, Shankaraghatta, Shivamogga, Karnataka 577451, India

Received: 8 March 2024 / Accepted: 12 May 2024
© The Author(s) 2024

Abstract This study introduces a pioneering approach to analyzing compact stars through Finslerian geometry, which has not been previously explored in this context. By employing the Barthel connection within Finsler–Randers spaces, the research derives a novel metric for compact stars, utilizing the unique geometric nature of spacetime inherent in Finslerian geometry. This offers a fresh perspective on understanding the structure of these stars, departing from the traditional Riemannian geometry commonly used in astrophysics. Specifically, the investigation delves into the Randers metric within Finslerian geometry to investigate the dynamics of these celestial bodies. It defines a component of Randers space, denoted as $\eta(r) = a + \frac{br^2}{R^2}$, where a and b are constants, r represents radial distance, and R signifies the observed radius of the star. The research focuses on developing metric potentials within the Finslerian framework, enabling a comprehensive comparative analysis of their regularity. By leveraging the unique physical properties of compact stars, the study determines the values of constants “a” and “b,” as well as those associated with metric potentials. Through an analysis of four distinct compact stars, the research provides valuable insights into various physical attributes based on estimated data. Furthermore, the investigation explores thermodynamic quantities derived within the Finslerian framework, contributing to the characterization of these compact stars. The study emphasizes the stability inherent in the configuration of compact stars under Finsler space geometry, indicating the potential applicability of Finsler geometry in understanding and characterizing celestial bodies in astrophysics.

1 Introduction

Compact stars, recognized for their extraordinary density and small size, are the remnants of massive stars that have completed their nuclear fusion and undergone gravitational collapse. Within this celestial category, white dwarfs and neutron stars are observed. White dwarfs originate from stars of low to moderate mass, while neutron stars emerge from the cataclysmic explosions of supernovae in more massive stellar bodies. Additionally, a hypothetical class of compact stars exists—black holes—forming when massive stars collapse beyond the neutron star phase, resulting in an entity whose gravitational pull is so immense that not even light can escape. Research in this field of astrophysics delves into understanding the extremes of matter and gravity, providing invaluable insights. Furthermore, studying these compact stars is crucial not only for unraveling the dynamics within galaxies but also for understanding the broader evolution of the universe [1, 2]. Exploring these compact celestial entities extends to investigating their potential roles in phenomena such as the propagation of gravitational waves and their potential connections to the enigmatic forces of dark matter and energy that significantly influence the universe’s composition and evolution.

The Einstein field equations (EFE), being nonlinear differential equations, pose significant challenges in obtaining analytical solutions. However, under the assumption of spherical symmetry, various solutions have been derived for the universe. These solutions encompass the de Sitter solutions, Schwarzschild solutions (both exterior and interior), and Kerr solutions. Notably, entities like wormholes, black holes, and compact stars emerge as solutions to these complex equations. The gravitational equilibrium of perfect fluids has been a focal point in understanding the solutions to EFEs, as evidenced in [3]. Compact stars, in particular, stand as solutions within the gravitational field equations, depicting the phase

^a e-mail: praveenjayarama1998@gmail.com

^b e-mail: sknmurthy@kuvempu.ac.in (corresponding author)

^c e-mail: yashmath0123@gmail.com

when all thermonuclear energy sources within a sufficiently massive star have been depleted. They persist as remnants of continuous gravitational contraction and are characterized by the application of the interior Schwarzschild metric [4]. Research has delved into establishing constraints for stable compact stars in a thermodynamic equilibrium state, exploring limitations related to their density, mass, and anisotropic parameters, as outlined in [5]. These investigations are fundamental in understanding the stability and properties of these intriguing celestial bodies.

Einstein's theory of general relativity has been a cornerstone in understanding the universe's structure. Countless studies within the realm of general relativity (GR) have focused on unraveling the intricacies of compact fluid spheres [6–21]. These investigations have aimed to provide an understanding of the behavior and characteristics of compact stars within the framework of GR. Moreover, there has been significant interest in exploring the behavior of compact stars under modified gravitational theories. Research endeavors in this domain have expanded the scope beyond classical general relativity, investigating how deviations or modifications in gravitational theories influence the properties and behaviors of these dense celestial objects. This avenue of study has opened new pathways to understanding gravity's role in shaping the structure and dynamics of compact stars, offering potential insights beyond the confines of traditional Einsteinian gravity [22–27]. The study of compact stars using the Karmarkar condition has been other area of research in compact stars [28–30].

The study of the universe within the broader context of Finsler geometry [31–33] represents an intriguing avenue of research that expands beyond traditional Riemannian geometry [41–64]. Finslerian metrics, such as the Randers metric and Kropina metrics [38,39], have become pivotal tools in investigating the universe's properties from this alternative geometric standpoint. These metrics play a crucial role in formulating and interpreting the theories of relativity within the framework of Finsler geometry, enabling the derivation of field equations that describe the dynamics and structure of the cosmos [44–46]. One notable aspect illuminated by this approach is the comprehension of the universe's anisotropy across various Finslerian backgrounds [47,48]. Researchers have employed Finsler geometry to better grasp the inherent directional disparities or irregularities observed throughout the cosmos. Through this exploration, they aim to unravel the underlying mechanisms driving these directional variations, offering a unique lens through which to understand the fundamental principles of relativity and the nature of our universe. Furthermore, the cosmological dynamics derived from the Finsler structure of the universe diverge from those obtained through the Riemannian framework. This distinction is reflected in the physical equations formulated within the Finslerian context, offering a different perspective and set

of tools to explore and understand the fundamental structure and evolution of the universe [49–57].

The utilization of Finsler–Randers (FR) metrics has proven to be remarkably successful in elucidating various facets of the universe, encompassing the structure of space-time, the mechanisms behind inflation [54,55], and even the characteristics of compact celestial entities like wormholes [56–59] and compact stars [60,62]. These theories suggest that FR metrics serve as promising candidates for explaining observed universal phenomena. Moreover, they propose that the Finsler metric stands out as a metric for understanding both the isotropic and anisotropic structures within the universe, surpassing the capabilities of the traditional Riemannian metric.

The success of Finsler geometry in elucidating various aspects of the universe arises from its intricate geometric properties. Our current focus lies in investigating into the exploration of celestial objects, particularly compact stars, within the framework of FR backgrounds. In our research, we employ the Barthel connection [31–38], a significant tool within the study of Finsler spaces, to address and simplify these intricate geometries. Leveraging the osculating Riemannian approach [40], which aids in navigating the complexities inherent in Finsler spaces, we utilize the Barthel connection to streamline our analysis. This approach is the focus of ongoing research [54–56,63,64], where the application of such connections enables us to shed light on the dynamics of dark energy and the evolution of the universe within the framework of Finsler geometry. Our aim is to extend this approach further by elucidating the structure and properties of compact stars within the Finslerian background. By adopting these methodologies, we seek to unravel new insights into the nature of these dense celestial objects, leveraging the geometric richness of Finsler geometry to deepen our understanding of compact stars and their role within the broader cosmic landscape.

This paper is structured as follows: Sect. 2 provides a concise introduction to Finsler geometry and derives the metric tensor expression for the line element of compact stars. Additionally, it presents the expressions governing the thermodynamic properties of the fluid that forms these compact stars. Section 3 delves into the physical characteristics of these stars, validating different thermodynamic aspects and assessing their stability conditions. Finally, Sect. 4 explores the significant findings of this study and offers a comprehensive physical interpretation of the model investigated.

2 Fundamentals of Finsler geometry in compact star analysis

Finsler geometry [31–33], as the metric extension of Riemannian geometry without imposing quadratic restrictions,

encompasses a wide range of geometric objects within the tangent bundle of the manifold M of dimension n . Computing these objects poses significant challenges. To streamline our calculations, we utilize the Barthel connection by employing the path of the osculating Riemannian space. This approach simplifies the computation of geometric entities in terms of the Christoffel symbol. Essentially, this process allows us to reduce all spatial geometry to Riemannian space geometry, where the distinguishing factor lies in replacing the metric of Riemannian geometry with the osculating Barthel–Finsler–Randers metric [54–56,63,64]. This captures the inherent anisotropic nature of Finsler geometry, intricately embedded within the geometry of Finsler space.

We begin our exploration of compact stars within the framework of Finsler geometry. Finsler geometry inherently defines a metric function on the manifold M , denoted as F , on the tangent bundle of a differentiable manifold. This function F is instrumental in defining the Finslerian metric tensor, $g_{ij}(xy)$, represented by Eq. (1)

$$g_{ij}(x, y) = \frac{\partial^2 F^2}{\partial y^i \partial y^j} \tag{1}$$

and $(x, y) = (x^i, y^j)$ are the canonical coordinates of the tangent bundle with $y = y^i \frac{\partial}{\partial x^i}$ for any tangent vector y at $x \in M$. Additionally, $g_{ij}(xy)$ is homogeneous of degree zero in y^i .

In this study, we aim to apply the Barthel–Finsler–Randers space to elucidate the structural characteristics of anisotropic compact stars [19,20]. The Randers metric [38,39] comprises the combination of a Riemannian metric $\alpha(xy)$ and a differentiable 1-form $\beta(xy)$. Conventionally, the Riemannian structure represents an isotropic and spherically symmetric universe, while the 1-form β encapsulates directional-dependent anisotropy inherent in structures [47]. This Randers metric, as represented by Eq. (2), is formulated as

$$F(x, y) = \alpha(x, y) + \beta(x, y) = \sqrt{a_{ij}(x) y^i y^j} + B_i(x) y^i. \tag{2}$$

Here, the juggling of indices is carried out utilizing the Riemannian metric tensor $a_{ij}(x)$

2.1 Finslerian compact star model

For the study of compact stars or any stellar structure in the context of Finslerian structure, the general consideration of the metric function is of the form [46,60]

$$F^2 = B(r) y^t y^t - A(r) y^r y^r - r^2 \bar{F}^2(\theta \phi y^\theta y^\phi). \tag{*}$$

Here, the functions A and B are dependent on the radial distance r . And the dynamics of stellar objects have been derived using this metric [57,59–62] But in the present work,

we have proposed a new metric for the study of stellar objects, which we now describe in detail.

The line element describing the spacetime around a static, spherically symmetric matter distribution in Schwarzschild coordinates is written as [5,16–21]

$$ds^2 = e^{v(r)} dt^2 - e^{\lambda(r)} dr^2 - r^2 d\theta^2 - r^2 \sin^2 \theta d\phi^2. \tag{3}$$

Here, $v(r)$ and $\lambda(r)$ are called metric potentials (gravitational component functions) and are functions of radial distance r . This equation characterizes the structure of spacetime around a spherically symmetric mass, incorporating elements for time, radial distance, and angular coordinates. In this particular context, we are considering the Riemannian metric of a Randers metric as

$$\alpha(x, y) = ds^2 = \text{diag} \left(e^{v(r)}, -e^{\lambda(r)}, -r^2, -r^2 \sin^2 \theta \right). \tag{4}$$

For $\beta(x, y)$, it is expressed as a vector

$$\beta(x, y) = B_i y^i, \tag{5}$$

where $B_i = (\gamma(r), 0, 0, 0)$ is a vector with components $(\gamma(r), 0, 0, 0)$, and (y^i) represents the coordinates $(y^i) = (y^0, y^1, y^2, y^3) = (t, r, \theta, \phi)$. By incorporating the Barthel connection and considering that 1-form $\beta(x, y)$ has a nonzero time component within compact stars, using Eqs. (2)–(5) in Eq. (1), we derive the osculating FR metric with the approach as in [54–56,63,64], and detailed derivation has been given in the Appendix.

$$(g_{ij}(x, y)) = \text{diag} \left(\eta(r) (e^{v(r)} + \eta(r) - 1), -\eta(r) e^{\lambda(r)}, -\eta(r) r^2, -\eta(r) r^2 \sin^2 \theta \right), \tag{6}$$

with $\eta(r) = \gamma(r) + 1$.

This metric describes the geometry of spacetime, accounting for the influence of the time-dependent factor $\gamma(r)$ within compact stars, modifying the elements of the metric tensor accordingly. And this metric structure clearly differs from the metric equation of compact stars as referred in [46,60].

In the context of the osculating Riemannian approach [34,40] and the Barthel connection, when transitioning from Finslerian geometry to Riemannian geometry, the Finslerian connections and curvatures can be expressed in terms of the Riemannian Christoffel symbols. This transition allows the Finslerian form of the EFEs to essentially transform into EFEs within Riemannian geometry. The distinction lies in the replacement of Riemannian metric components with Finslerian metric components, characterized by the inclusion of an anisotropic term denoted as $\eta(r)$. Consequently, the EFEs take the form

$$G_{ij} = R_{ij} - \frac{1}{2} R g_{ij} = k T_{ij}, \tag{7}$$

where $k = \frac{8\pi G}{c^4}$ with G is the Newtonian gravitational constant, and c is the speed of light. For this specific work, k has been set to 1, g_{ij} is the osculating FR metric, and T_{ij} is the energy momentum tensor that characterizes the anisotropic matter distribution (perfect fluid) within the compact stars and is of the form [20–23,23,24]

$$T_j^i = (\rho + p_t) u^i u_j - p_t \delta_j^i + (p_r - p_t) v^i v_j \tag{8}$$

with $u^i u_j = -v^i v_j = 1$; $u^i v_j = 0$. Here, u_i is the four-velocity vector, v_i represents unit radial vector, ρ is the energy density, p_r is the radial pressure measured in the direction of u_i , and p_t is the transverse pressure of the matter that is fluid content distributed in compact stars, which is measured in an orthogonal direction to v_i . Thus, the components of the T_{ij} are given by

$$T_{ij} = \text{diag} (\rho g_{00}, -p_r g_{11}, -p_t g_{22}, -p_t g_{33}). \tag{9}$$

Therefore, the EFEs of line element (6) along with (9) lead to the following set of independent equations:

$$\rho = \frac{e^{v-\lambda} \left(r \left(\eta' r + 2\eta \right) - 4r\eta' - 2\eta \right)}{2r^2\eta^2 (e^v + \eta - 1)} + \frac{e^{-\lambda} (\eta - 1) \left(r \left(\eta' r + 2\eta \right) \left(\lambda' - 4\eta' r - 2\eta \right) + 2\eta (e^v + \eta - 1) \right)}{2r^2\eta^2 (e^v + \eta - 1)}, \tag{10}$$

$$p_r = \frac{e^{\lambda-v} \left(\left(v' r^2 + 4r \right) \eta' + 2v' \eta r + 2\eta \right) + 2e^{-\lambda} \left(r \left(3\eta - 2 \right) \eta' + \eta^2 - \eta \right) - 2\eta (e^v + \eta - 1)}{2r^2\eta^2 (e^v + \eta - 1)}, \tag{11}$$

$$p_t = \frac{e^{-\lambda}}{2r \left(e^{2v(r)} + (\eta(r) - 1) (\eta(r) + 2e^{v(r)} - 1) \right) \eta(r)^2} \left[\left(\left(\eta v'' - \lambda' \left(\eta + \frac{v'}{2} r + r\eta' \right) \right) + \frac{(\eta v' + 2\eta') (v' + 2)}{2} \right) e^{2v} + \eta e^v r (\eta - 1) v'' + \left(-v' e^v r + (5\eta - 4) e^v + 3\eta^2 - 5\eta + 2 \right) \eta' + \frac{\lambda' \left(-3r\eta' \left(\frac{2}{3} + \frac{(5\eta-4)e^v}{3} + \eta^2 - \frac{5\eta}{3} \right) - \eta (\eta - 1) (v' e^v r + 2\eta + 4e^v - 2) \right)}{2} + v' e^v \eta (\eta - 1) (v' r + 1) \right] \tag{12}$$

where the prime denotes the radial derivative of the functions.

In the context of solving the EFEs for anisotropic compact stars within the FR geometry, the system of Eqs. (10)–(12) involves six unknowns: ρ , p_r , p_t , v , λ , η . To solve this system, choices or approximations for three variables need to be made. Researchers often employ various approximations for variables such as $v(r)$ and $\lambda(r)$ to discuss the structure of compact stars among all these metric potentials in this work. The expressions chosen for the variables are [22–24]

$$v(r) = Br^2 + C, \tag{13}$$

$$\lambda(r) = Ar^2. \tag{14}$$

Here, A , B and C are arbitrary constants determined by certain physical assumptions. These expressions are selected to

ensure a structure of compact stars without singularities. The variable $\eta(r)$ plays a crucial role in the solutions of the EFEs. An expression for $\eta(r)$ is suggested as

$$\eta(r) = a + \frac{br^2}{R^2}. \tag{15}$$

Here, a and b are real constants, and R is a characteristic radius of the compact stars. This expression for $\eta(r)$ is proposed based on specific considerations, likely tied to the desired properties of the spacetime geometry and matter distribution within compact stars. Choosing appropriate expressions for $v(r)$, $\lambda(r)$ and $\eta(r)$ is crucial in finding solutions to the EFEs and ensuring the physical validity of the resulting model for compact stars within the FR background. These choices are often guided by physical intuition, observations, and desired properties of the spacetime metric.

When selecting the expressions for $v(r)$, $\lambda(r)$ and $\eta(r)$ in the context of solving the EFEs for compact stars within the FR geometry, several considerations come into play, which are as follows[25–30]:

1. Singularity avoidance: The expressions for $v(r)$, $\lambda(r)$ and $\eta(r)$ as $Br^2 + C$, Ar^2 , $\eta(r) = a + \frac{br^2}{R^2}$ are chosen to ensure a singularity-free structure for compact stars. These choices are motivated by the desire to create physically plausible solutions without encountering problematic singularities in the spacetime.
2. Physical relevance The parameters A , B , C , a , and b are determined based on physical assumptions and constraints derived from observed behaviors in stellar structures. These constants encapsulate properties such as mass distribution, energy density profiles, or conditions within compact stellar objects.
3. Metric structure: The form of the metric tensor g_{ij} in Eq. (6) is instrumental in defining the geometry around

compact stars within the FR background. The expression for $\eta(r)$ as $a + \frac{br^2}{R^2}$ plays a crucial role in characterizing the anisotropic effects within this metric structure derived in a Finslerian background

- Anisotropic influence of $\eta(\mathbf{r})$: $\eta(r)$ is a component of the smooth vector field β , which is nonvanishing on the manifold M . This 1-form β introduces anisotropy into the metric, allowing for directional dependence and nonuniform behavior within the compact star. It must be a smooth function defined on the manifold and must be nonvanishing; otherwise, the metric reduces to a Riemannian one. Therefore, we have selected $\eta(r)$ to be a nonvanishing analytic function defined on M . Different forms of $\eta(r)$ can be chosen to ensure the validity of the proposed metric structure. These choices are guided by physical intuition, empirical observations, and desired properties of the spacetime metric. Specifically, the expression for $\eta(r)$ is chosen to satisfy the condition $\eta(R) = 1$. This condition ensures that our metric structure resembles the Schwarzschild metric when matched at the boundary of the compact stars. The term $\eta(r)$ introduces anisotropic effects into the spacetime metric, allowing for nonuniform behavior in different spatial directions. The constants a and b in Eq. (15) potentially control how anisotropy varies with radial distance and might influence the overall geometry and matter distribution within compact stars. The presence of R in the denominator of the term η likely indicates a characteristic scale for anisotropy. This parameter might govern the extent or range over which the anisotropic effects become significant within the spacetime of compact stars. And we point

out that this $\eta(r)$ may be the additional field or energy that keeps the stability of the compact stars. Thus, this Finslerian term may contribute additional stability to compact structures, and it may be the cause for dark energy or any form of other energy that may be present within the structure of compact stars.

Physical implications

- The choice of these expressions aims to reflect physical properties and behaviors observed or theorized within compact stellar structures.
- The specific values of the constants (A, B, C, a, b) are typically determined through analysis and calculations based on physical models, observations, or phenomenological considerations.
- This choice for $\eta(r)$ allows us to incorporate anisotropic effects that vary with radial distance. The term $\frac{br^2}{R^2}$ introduces dependence on r , indicating how anisotropic effects evolve with distance from the center of the compact star. The constant a represents a baseline anisotropy, while the term $\frac{br^2}{R^2}$ adds a radial dependence to the anisotropic effects.

These choices and expressions form the foundational assumptions necessary to proceed with solving the EFEs and ultimately derive solutions describing the structure of compact stars within the FR geometry.

Thermodynamic parameters

By substituting the expressions (13)–(15) in EFEs, we have the expression for ρ, p_r, p_t as

$$\rho = \frac{2R^2 \left(\left(a \left(Ar^2 - \frac{1}{2} \right) R^2 + 2r^2b \left(Ar^2 - \frac{5}{4} \right) \right) R^2 e^{(-A+B)r^2+C} + \frac{R^2(aR^2+br^2)}{2} e^{Br^2+C} \right)}{\left(e^{Br^2+C} R^2 + (a-1) R^2 + br^2 \right) r^2 (aR^2 + br^2)^2} + \frac{2R^2 \left((a-1) R^2 + br^2 \right) \left(\left(a \left(Ar^2 - \frac{1}{2} \right) R^2 + 2r^2b \left(Ar^2 - \frac{5}{4} \right) \right) e^{-Ar^2} + \frac{ar^2}{2} + \frac{br^2}{2} \right)}{\left(e^{Br^2+C} R^2 + (a-1) R^2 + br^2 \right) r^2 (aR^2 + br^2)^2}, \tag{16}$$

$$p_r = \frac{2R^2 \left(\left(a \left(Br^2 + \frac{1}{2} \right) R^2 + 2r^2b \left(Br^2 + \frac{5}{4} \right) \right) R^2 e^{(-A+B)r^2+C} - \frac{R^2(aR^2+br^2)}{2} e^{Br^2+C} \right)}{\left(e^{Br^2+C} R^2 + (a-1) R^2 + br^2 \right) r^2 (aR^2 + br^2)^2} + \frac{2R^2 \left(\left(\frac{(a^2-a)R^2}{2} + 4r^2b \left(a - \frac{5}{8} \right) R^2 + \frac{7}{2}b^2r^4 \right) e^{-Ar^2} - \left((a-1) R^2 + br^2 \right) (aR^2 + br^2) \right)}{\left(e^{Br^2+C} R^2 + (a-1) R^2 + br^2 \right) r^2 (aR^2 + br^2)^2}, \tag{17}$$

Table 1 Observed physical properties of compact stars

Name of compact star	m (mass)	R (radius)
Her X-1	$m = 0.85$	$R = 8.1$
Cen X-3	$m = 1.74$	$R = 11.751$
PSR J1416-2230	$m = 1.97$	$R = 12.182$
SMX X-1	$m = 1.04$	$R = 10.067$

exterior metric in a Finsler background, which extensively depends upon the velocity vector y^i . But in the present work, metric equation (6) represents an osculating Finsler–Barthel–Randers metric defined on the tangent space of the manifold. Due to the fundamental differences in the form and dependencies of our interior metric and the ansatz-based exterior metric in Ref. [46], a direct comparison is not straightforward. Thus, in order to compare the obtained metric Eq. (6)

$$\begin{aligned}
 p_t = & -\frac{e^{Ar^2} R^2}{e^{2Br^2+2C} R^4 + (2R^2 e^{Br^2+C} + (a-1) R^2 + br^2) ((a-1) R^2 + br^2) (aR^2 + br^2)^2} \\
 & \times \left\{ \left(R^4 \left(a \left(B(A-B)r^2 + A - 2B \right) \right. \right. \right. \\
 & \left. \left. \left. + B(A-B)r^4 + (3A-4B)r^2 \right) \right) e^{2Br^2+2C} + \left((a-1)a(B-2B)r^2 + 2A - 2B \right) r^2 \right. \\
 & \left. + 2A - 2B \right) R^4 + r^2 b^2 \left(-5 + B(A-2B)r^4 + (7A-2B)r^2 \right) R^2 e^{Br^2+C} + \left(Aa(a-1) R^4 \right. \\
 & \left. + 5b \left(A \left(a - \frac{5}{3} \right) r^2 - \frac{3a}{5} + \frac{2}{5} \right) R^2 + \left(4Ar^4 - 3r^2 \right) b^2 \right) \left((a-1) R^2 + br^2 \right) \right\}. \tag{18}
 \end{aligned}$$

Exploring anisotropic compact star models within Finslerian geometry involves considering theoretical properties for compact stars like Her X-1, Cen X-3, PSR J1416-2230, and SMX X-1 [28]. Theoretical mass and radius details, listed in Table 1 and are utilized to refine and validate theoretical models against expected astrophysical behaviors. Incorporating these theoretical properties helps align predictions in Finslerian geometry with stellar characteristics.

3 Physical characteristics of solutions for compact stars

3.1 Matching conditions

In the process of determining the constants A , B , C , a , and b within the metric function, it is crucial to note that we encounter five unknowns constrained by three equations. To resolve this, we leverage the concept of matching conditions, ensuring equivalence between the interior and exterior geometries of anisotropic stars. The principle of matching boundary conditions dictates that the geometric structure of a star, whether observed internally or externally, should not influence the interior boundary metric. This means that regardless of the chosen metric, its components must exhibit continuity at the boundary, maintaining consistency across the entire structure without being impacted by specific metrics or observations.

When dealing with self-gravitating compact stars, the Schwarzschild metric characterizes the outer exterior geometry, defining the spacetime around the star, whereas in the case of [46] utilizing the proposed metric, they have derived the

with the exterior metric, we proceed as follows. The metric, given by Eq. (19), is reliant on the mass M and radius r of the compact star, where $r > 2M$, and it represents the exterior metric in the Riemannian case [3, 20–23],

$$\begin{aligned}
 ds^2 = & \left(1 - \frac{2M}{r} \right) dt^2 - \left(1 - \frac{2M}{r} \right)^{-1} dr^2 \\
 & - r^2 d\theta^2 - r^2 \sin^2 \theta d\phi^2. \tag{19}
 \end{aligned}$$

In the process of matching the interior metric to the vacuum exterior solution at the boundary surface $r = R$, smooth continuity conditions are crucial. These conditions, outlined in Eq. (19), ensure consistency between the interior and exterior metrics at the boundary, maintaining smooth transitions between them.

$$\begin{aligned}
 e^{v^-} |_{r=R} &= e^{v^+} |_{r=R}, \quad e^{\lambda^-} |_{r=R} = e^{\lambda^+} |_{r=R}, \\
 \left(\frac{\partial e^{v^-}}{\partial r} \right) |_{r=R} &= \left(\frac{\partial e^{v^+}}{\partial r} \right) |_{r=R} \\
 g_{rr}^- (R) &= g_{rr}^+ (R), \\
 g_{tt}^- (R) &= g_{tt}^+ (R), \quad \frac{\partial g_{tt}^-}{\partial r} = \frac{\partial g_{tt}^+}{\partial r}. \tag{20}
 \end{aligned}$$

However, the derived FR metric for the compact star involves the presence of the special term $\eta(r)$ within the metric equation (6). To ensure seamless matching between this anisotropic metric and the Schwarzschild metric (19), a condition is chosen at the boundary $r = R$

$$\eta(R) = 1. \tag{21}$$

The condition (21) is chosen specifically to align the anisotropic metric with the Schwarzschild metric at the

boundary. This choice not only guarantees the matching of these metrics but also introduces an important constraint, $a + b = 1$. This constraint emerges from Eq. (21), effectively linking the values of the unknown constants a and b governing the anisotropic metric. By utilizing Eq. (21) and enforcing the continuity of metric potentials, further constraints on the unknown parameters can be derived. This step is key in ensuring a smooth transition and match between the interior anisotropic metric and the exterior Schwarzschild metric at the boundary of the compact star.

Ultimately, these conditions and constraints are influential in harmonizing the anisotropic interior metric, characterized by the presence of $\eta(r)$, with the vacuum exterior Schwarzschild metric, creating a smooth and consistent transition at the boundary of the compact star. Thus, we have,

$$A = \frac{1}{R^2} \log\left(\frac{R}{R - 2M}\right), \tag{22}$$

$$B = \frac{m}{R^3 \left(1 - \frac{2m}{R}\right)}, \tag{23}$$

$$C = \log\left(\frac{R - 2m}{R}\right) - \frac{m}{R \left(1 - \frac{2m}{R}\right)}. \tag{24}$$

To evaluate the unknown constants A, B, C, a, b within the Eqs. (16)–(19), the expressions for A, B, C are substituted accordingly. To determine a and b , standard values of m and R for different compact stars are employed, utilizing the relation $a = 1 - b$. Using the boundary condition $p_r = 0$ at $r = R$, that is, at the boundary of the stars, the radial pressure drops [20,28], and we obtain the expression for b as

$$b = \frac{-2BR^2 e^{(-A+B)R^2+C} + e^{BR^2+C} - e^{(-A+B)R^2+C}}{2BR^2 e^{(-A+B)R^2+C} + 2e^{-AR^2} + 4e^{(-A+B)R^2+C}} \tag{25}$$

Once the values of A, B, C, b are derived from these equations, their substitution with the known mass m and radius R values of the stars help calculate these five unknown constants, as detailed in Table 2. This computation is followed by the determination of thermodynamic parameters such as density and pressure terms using the Friedmann equation. The subsequent discussion centers on interpreting the outcomes obtained from the proposed anisotropic star model and understanding their physical implications in the context of these compact stars.

In this study, the stars Her X-1, Cen X-3, PSR J1416-2230, and SMX X-1 have been denoted as CS1, CS2, CS3, and CS4, respectively [28]. This nomenclature allows for a streamlined and concise reference to these specific compact stars throughout the research work.

Astrophysical behavior and characteristics of compact stars

Validating the proposed model involves confirming key physical conditions known to be essential for anisotropic fluid stellar systems. Some of these crucial conditions typically considered include the following analysis:

1. Singularity analysis: Examining whether the model predicts the presence or absence of singularities within the stellar structure. Identifying and understanding the nature of these singularities is pivotal in determining the validity of the model.

2. Energy conditions: Ensuring that the energy conditions such as the null, weak, strong, and dominant energy conditions play a vital role in characterizing the behavior of energy–momentum tensors within the model.

3. Causality conditions: Verifying that causality is preserved within the model, meaning that no signal or information travels faster than the speed of light. This is fundamental in maintaining the integrity of causal relationships.

4. Stability and perturbations: Investigating the stability of the model against perturbations. It is crucial to ascertain whether small disturbances lead to amplified effects or if the system remains stable.

5. Mass–radius constraints: Comparing the predicted mass and radius of the compact stars within the model against observed or theoretically established constraints. Ensuring these properties align within acceptable ranges adds credibility to the model.

6. Causality and causation constraints: Verifying that causality is maintained, and the model adheres to the causal nature of physical laws. This involves analyzing the temporal and causal relationships within the stellar system.

7. Physical equilibrium: Confirming that the model represents a physically plausible equilibrium state for compact stars, ensuring that the forces within the system balance each other satisfactorily.

These conditions are crucial benchmarks in validating the physical realism and consistency of the proposed anisotropic fluid stellar model. Verifying these conditions helps in establishing the credibility and applicability of our model within the realm of astrophysical phenomena and are discussed as below.

3.2 Metric regularity and comparative analysis: Riemannian and Finslerian geometries

For the metric to be regular, the metric potentials must meet specific criteria: they should remain positive, finite, and free of singularities within the star’s interior. Additionally, at the central point $r = 0$, the metric functions should adhere to $e^{\nu(0)} = \text{constant}$ and $e^{-\lambda(0)} = 1$, which corresponds to the Riemannian case when $\eta(r)$ equals 1 in the metric (6).

Table 2 Values of physical constants for four different compact stars

Compact star	A	B	C	b
Her X-1	0.003590398893	0.002024272214	-0.3683785716	4.713362070 10^{-11}
Cen X-3	0.002543218860	0.001523496900	-0.5615565171	-8.338427832 10^{-11}
PSR J1416-2230	0.002632840029	0.001610632379	-0.6297360751	-1.249068717 10^{-10}
SMX X-1	0.002283770241	0.001284841387	-0.3616591215	0.0000277286033

Maintaining the regularity condition for our (FR) metric necessitates the regularity of $\eta(r)$ across the star's interior. The chosen form of $\eta(r)$ from the expression (21) remains regular throughout the interior, as it represents a simple analytic function in r . Additionally, it is shown that $(\eta(r)e^{v(r)})'_{r=0} = (\eta(r)e^{\lambda(r)})'_{r=0} = 0$, further confirming the regularity of the metric potentials at the stellar center. To offer a comparative perspective between Riemannian and Finsler geometry through the metric potentials, we have plotted these potentials for $\eta(r) = 1$ and $\eta(r) = a + \frac{br^2}{R^2}$, as depicted in Fig. 1a and b. These plots substantiate the regularity of the FR metric components g_{tt} and g_{rr} . In the Finslerian case, we have taken $v'(r) = (\eta(r)(e^{v(r)} + \eta(r) - 1)\lambda'(r) = \eta(r)e^{\lambda(r)}$, as indicated in Fig. 1b. These analyses emphasize the regular behavior of the metric functions and their adherence to physical regularity criteria within the context of the proposed anisotropic model for compact stars.

3.3 Characteristics of energy density and pressure profiles

In a valid model, energy densities and pressures need to meet specific criteria. Inside the star, they should stay non-negative and finite at the center: $\rho_0 = \rho(0)$ and $p_{r0} = p_r(0)$. Moreover $\rho_0 = p_{r0}$, as evident in Fig. 2. Energy density peaks at the radius and decreases uniformly towards the star's edge. Pressure components, radial p_r and tangential p_t , are pivotal for the star's stability. They reach maximum values at the core and taper off outwardly. Radial pressure vanishes at the star's boundary, defining the fluid sphere's limit.

For stability, these quantities should peak at the center finite $\rho_0 = \rho(0)$ and $p_{r0} = p_r(0)$. Moreover, $\rho_0 = p_{r0}$ and decreases outward, and $\rho' \leq 0$, $p'_r \leq 0$, $p'_t \leq 0$, and $\rho''|_{r=0} < 0$, $p_r|_{r=0} < 0$, $p_t|_{r=0} < 0$. Figure 2 shows gradients, starting at zero at the core and becoming negative towards the star's boundary, confirming model stability. The fact that energy density and pressure reach maximum values at the core and reduce outward suggests stability within the stellar structure. Additionally, the negative gradients of these quantities from the core to the boundary reinforce the stability of the model, indicating a balanced distribution of internal forces. The gradients of energy density and pressure components illustrate how these quantities change concerning radial

distance. Starting from zero at the star's center, their negative values outward indicate a decreasing trend, indicative of a stable and well-distributed pressure–energy profile.

3.4 The energy conditions

Ensuring adherence to specific energy conditions is crucial for verifying the validity of the matter content within the anisotropic distribution of compact stars. These conditions define the acceptability and viability of the matter mathematically and are known to characterize exotic matter content within compact stars.

- Strong energy conditions (SEC) if $\rho + p_j \geq 0$, $\rho + \sum_j p_i \geq 0, \forall j$
- Dominant energy conditions (DEC) if $\rho \geq 0$, $\rho \pm p_j \geq 0, \forall j$
- Weak energy condition (WEC) if $\rho \geq 0$, $\rho + p_j \geq 0, \forall j$
- Null energy condition (NEC) if $\rho + p_j \geq 0, \forall j$.

Figure 3 confirms that these energy conditions are met, validating the physical parameters' compliance with these conditions. This adherence implies that the matter distribution within the compact star aligns with normal fluid characteristics, complying with these energy conditions. This is a significant affirmation of the physical validity of the matter distribution within the compact star

3.5 Anisotropic parameter

The anisotropic parameter defined as in Eq. (26) is crucial for a stable compact star configuration. It determines the balance between radial and tangential pressures, where tangential pressure should surpass radial pressure, ensuring $\Delta > 0$

$$\Delta = p_t - p_r. \quad (26)$$

A positive Δ indicates an attractive anisotropic force, similar to quintessence, and signifies model compatibility and stability. In our study (Fig. 4), Δ starts at zero at the star's core and consistently increases toward the boundary, indicating an outwardly repulsive anisotropic force. This force prevents collapse, making compact stars stable structures [11]. The presence of this outward force ensures stability, suggesting

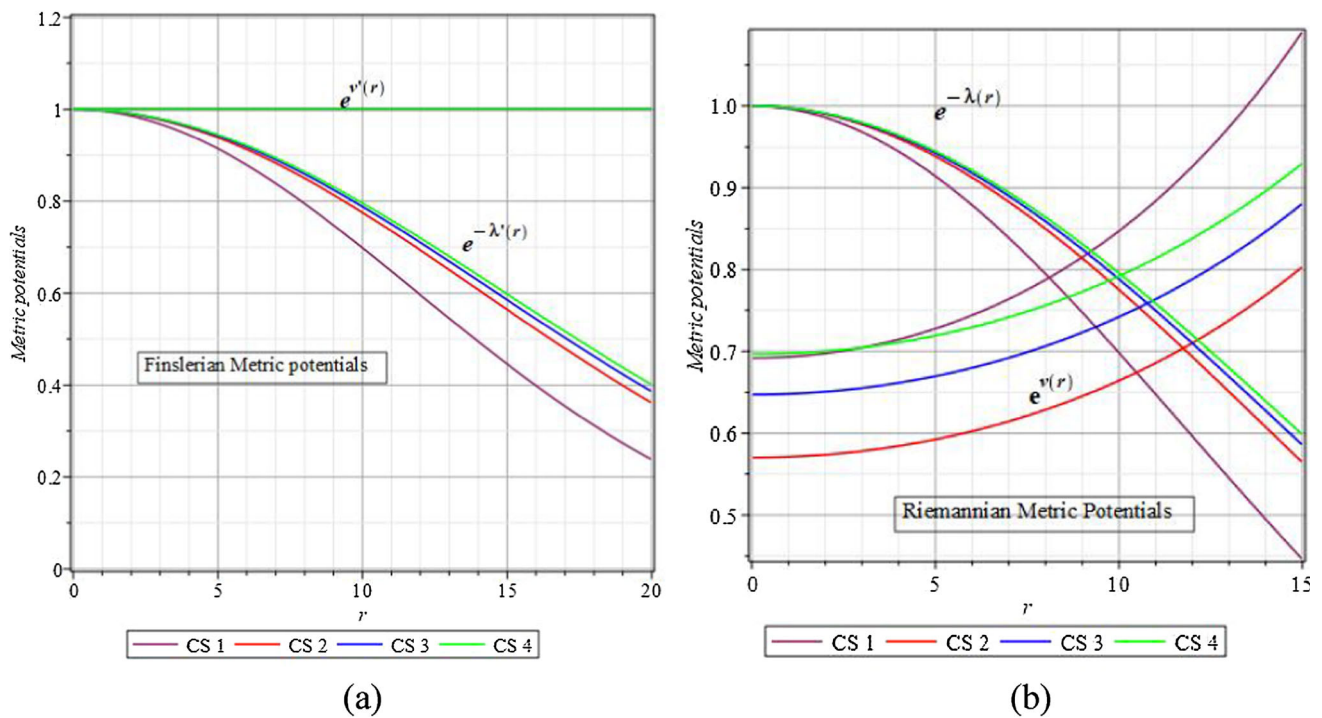


Fig. 1 **a** Metric potentials in the Finslerian context. **b** Metric potentials in the Riemannian context (with $(r) = 1$)

that compact stars rely on anisotropic forces to resist collapse rather than isotropic forces.

3.6 Equation of state parameter

The equation of state (EoS) parameters ω_r and ω_t determine the relationship between density and pressure in stable compact stars. They are defined as

$$\omega_r = \frac{p_r}{\rho}, \quad \omega_t = \frac{p_t}{\rho}. \tag{27}$$

For a physically feasible matter content, the graphical representation of EoS parameters (ω_r and ω_t) must fall within the range of 0–1. The maximum value of 1 signifies a non-exotic nature of the matter content within the stars. In our study, represented in Fig. 5, both ω_r and ω_t fall within the interval [0, 1] throughout the boundaries of the compact stars. This observation confirms that the fluid distribution comprises non-exotic matter, indicating a physically plausible matter content within the compact stars.

3.7 Herrera cracking method

Stability in the context of stellar structures is crucial for ensuring physical consistency and reliability. Herrera proposed a method, known as the cracking approach, to assess stability by analyzing the difference in sound speeds in radial and transverse directions [9]. According to Herrera’s criterion, the square of the sound speed, $v_s^2 = \frac{dp}{d\rho}$, must fall

within the [0, 1] interval to denote a physically stable stellar object. In an anisotropic compact star model, we consider two sound speeds, $v_{rs}^2 = \frac{dp_r}{d\rho}$ and $v_{ts}^2 = \frac{dp_t}{d\rho}$, representing the radial and tangential directions, respectively. For stability, both v_{ts}^2, v_{rs}^2 should adhere to the causality condition, lying between 0 and 1. In our study, as shown in Fig. 6, it is evident that the causality condition is met, confirming that the model complies with stability criteria. This observation reinforces the stability of our structured model for anisotropic compact stars, assuring their physical validity and structural robustness against external fluctuations.

Stability in self-gravitating anisotropic fluid spheres hinges on the relationship between radial and tangential sound velocities [10]. When $|v_{sr}^2 - v_{st}^2|$ lies between 0 and 1, it signifies a potentially stable configuration. In our study, as indicated in plot (7), the range $-1 \leq v_{ts}^2 - v_{rs}^2 \leq 1$ is observed, upholding the stability of our well-structured compact stellar model. This relationship between sound velocities indicates that the radial sound velocity surpasses the tangential one, ensuring the stability of the self-gravitating anisotropic fluid sphere. The model’s adherence to this stability criterion reflects its robust and stable configuration, and physical validity (Fig. 7).

3.8 Adiabatic index

The adiabatic index Γ serves as a metric for the rigidity of the equation of state (EoS) in an anisotropic fluid, denoting

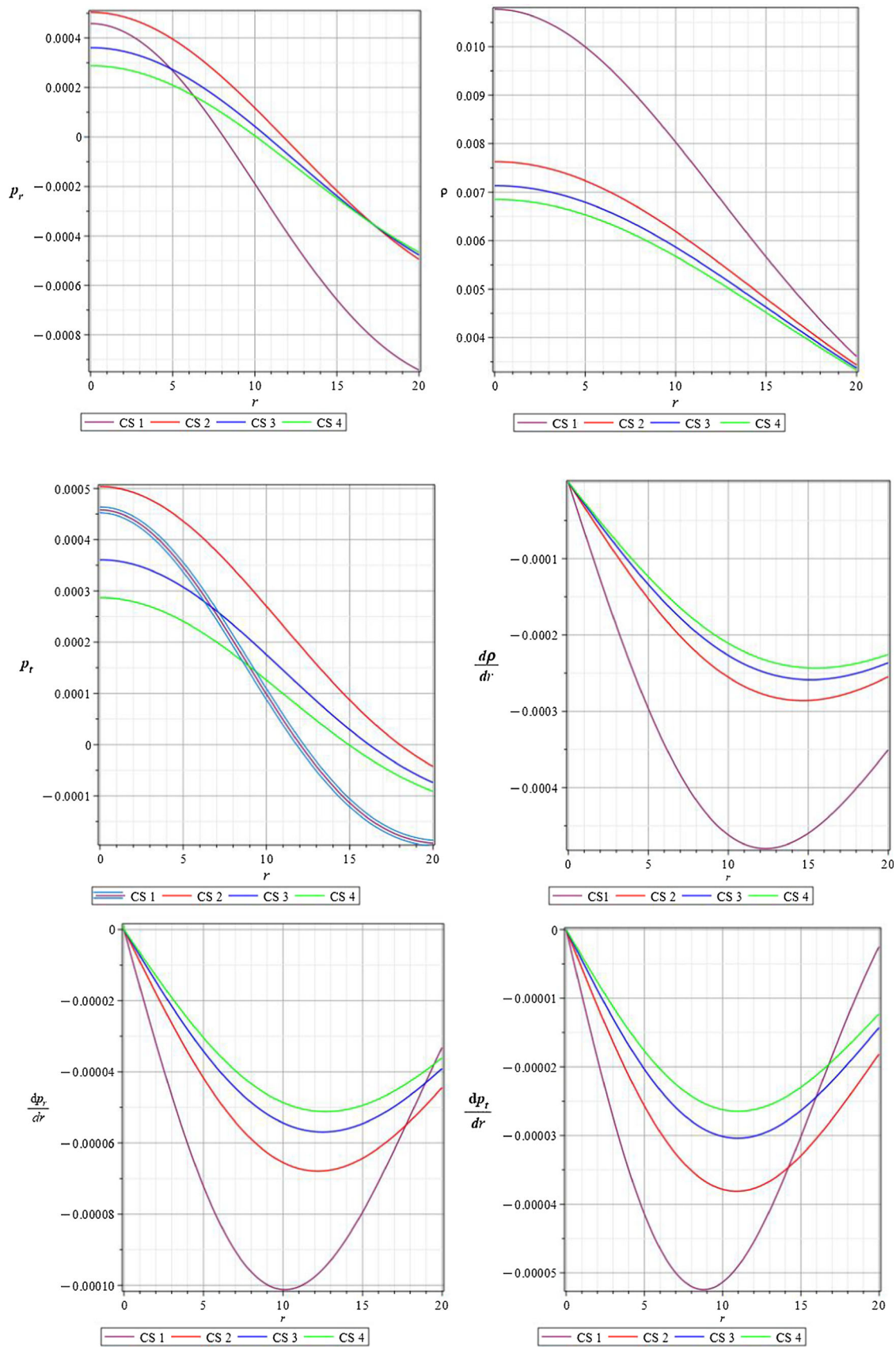


Fig. 2 Visualization of energy densities, pressure profiles, and gradients within compact stars

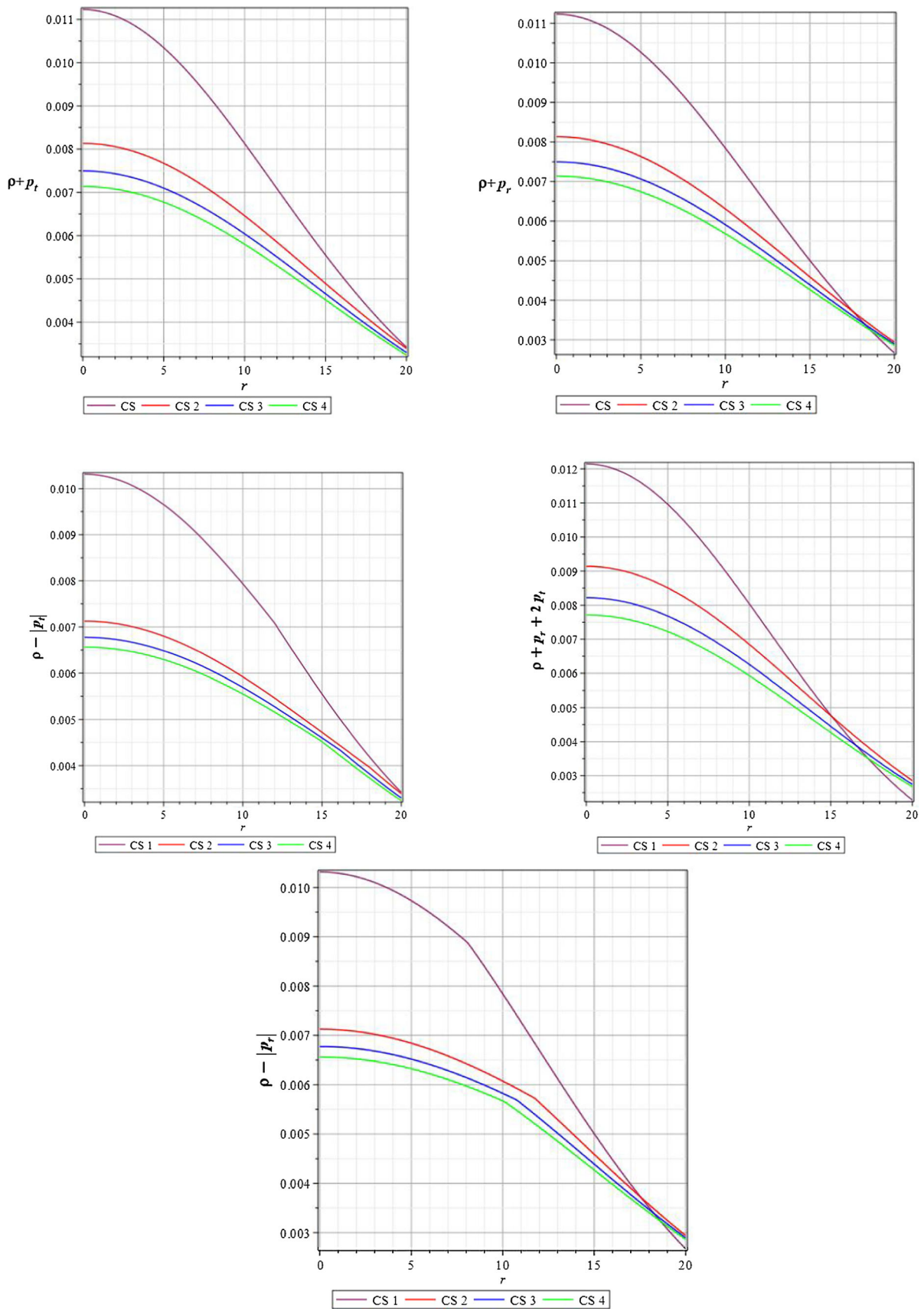


Fig. 3 Assessment of energy conditions in four compact stars

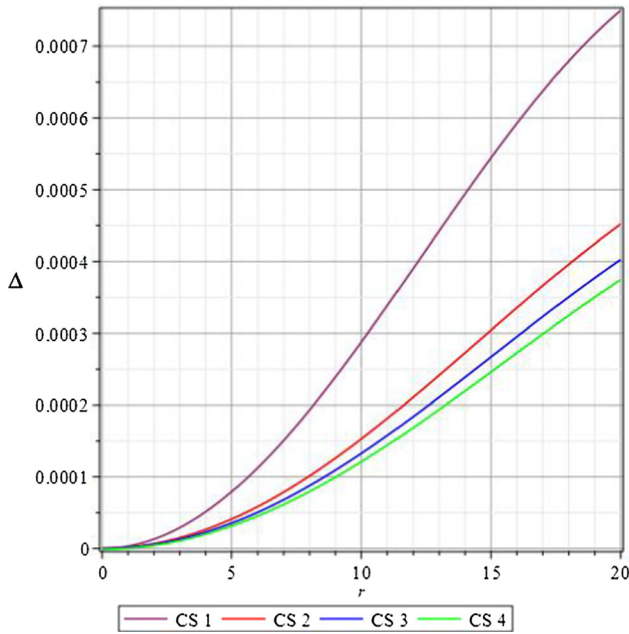


Fig. 4 The behavior of anisotropic parameters of four different compact stars

how pressure changes with minor shifts in matter density [7]. It is calculated using

$$\Gamma = \left(1 + \frac{\rho}{p_r}\right) \left(\frac{dp_r}{d\rho}\right). \tag{28}$$

Significant to stability is $\Gamma > \frac{4}{3}$, ensuring resilience against infinitesimal radial adiabatic perturbations. A higher Γ indi-

cates increased pressure change per unit energy density shift, illustrating a stiffer EoS. From Fig. 8, it is evident that Γ consistently exceeds $\frac{4}{3}$, affirming the model’s stability. This alignment implies its ability to resist collapse under radial adiabatic variations. A higher Γ denotes a stiffer equation of state, reflecting the model’s capacity to withstand compression and collapse, confirming its structural and physical consistency.

3.9 Stability under external forces

A star maintains a state of equilibrium under three distinct forces: gravitational force, hydrostatic force, and anisotropic force. Described by the Tolman–Oppenheimer–Volkoff (TOV) equation [3,4], this equation defines the internal structure of a spherically symmetric compact celestial body, initially formulated within the context of Riemannian geometry. Through the following calculations, we derive the FR TOV equation as follows:

$$\frac{(2\eta\eta' + e^v(\eta' + v'\eta) - \eta')}{\eta(e^v + \eta - 1)} (\rho + p_r) + \frac{dp_r}{dr} - \frac{2}{r} \Delta = 0. \tag{29}$$

The above expression can be written as

$$F_g + F_h + F_a = 0, \tag{30}$$

where

$$F_g = \frac{(2\eta\eta' + e^v(\eta' + v'\eta) - \eta')}{\eta(e^v + \eta - 1)} (\rho + p_r), \tag{31}$$

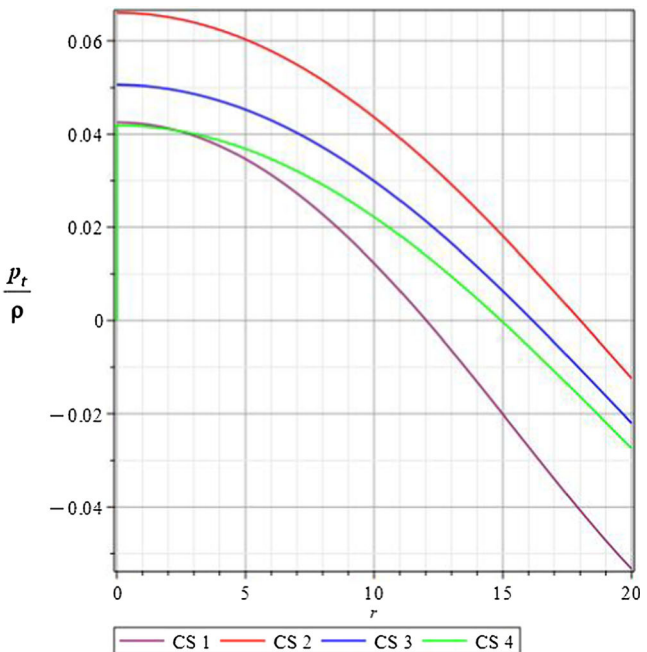
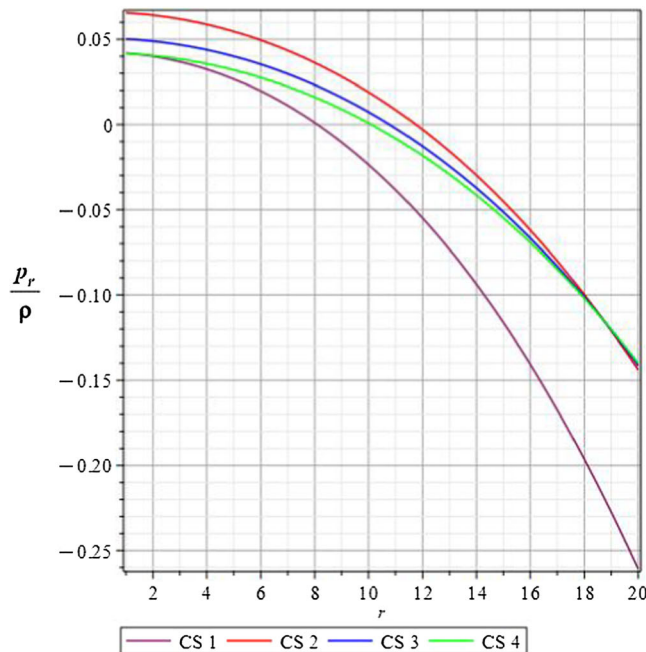


Fig. 5 EoS parameter behavior in four compact stars

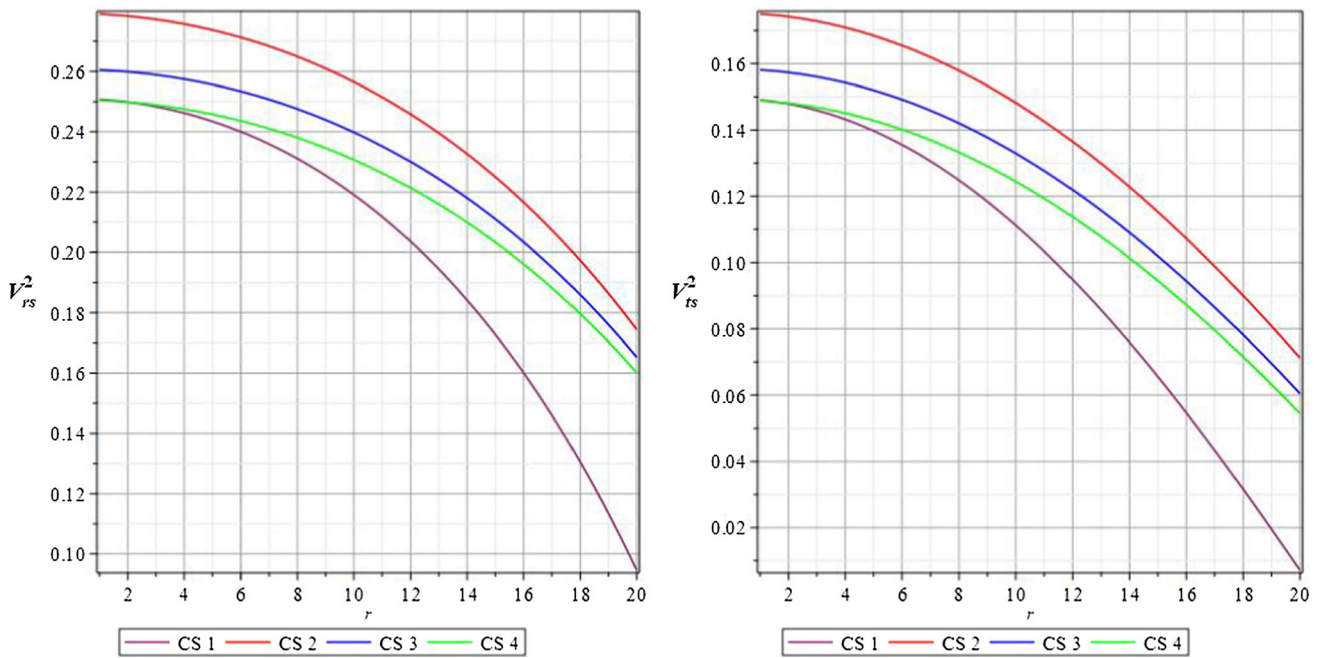


Fig. 6 Herrera’s cracking principle

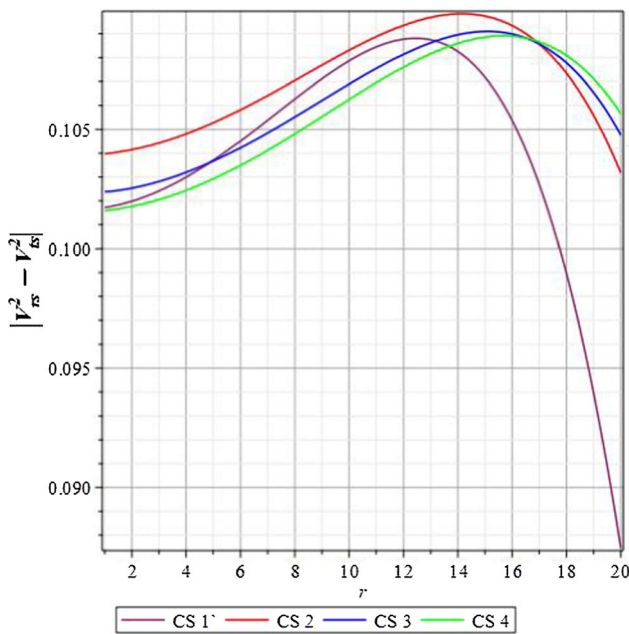


Fig. 7 Plot of $|v_{sr}^2 - v_{sr}^2|$

$$F_h = \frac{dp_r}{dr}, \tag{32}$$

$$F_a = -\frac{2}{r} \Delta. \tag{33}$$

Here, F_g , F_h , and F_a signify the gravitational, hydrostatic, and anisotropic forces, respectively.

This equation illustrates the equilibrium state of a fluid sphere due to the combined influence of these forces. Notably, as η approaches 1, this equation relapses to the Riemannian form. This suggests that Finslerian geometry’s impact on the gravitational field, referred to as Finslerian gravity, shapes the dynamics of stellar structures, influenced by the Finslerian term $\eta(r)$. The interplay of these forces is graphically depicted in Fig. 9. The presence of $\eta(r)$ introduces deviations from the standard Riemannian formulation, altering the behavior of the gravitational field within the star. In essence, the $\eta(r)$ term in the FR TOV equation signifies how Finslerian geometry introduces a directional dependence or anisotropic behavior within the gravitational field of the compact star. This provides a more detailed understanding of how geometry affects the dynamics and equilibrium conditions of such celestial objects.

3.10 Effective mass and compactness

The mass function, $m(r)$, within a radius r is calculated through the integral

$$m(r) = \int_0^r 4\pi r^2 \rho(r) dr. \tag{34}$$

It is essential to note that the density here is a function of $\eta(r)$. By substituting the expression for $\rho(r)$ into the above equation, the resulting expression for $m(r)$ becomes complex. This expression, depicted below, encapsulates various parameters and their dependence on the radial distance r :

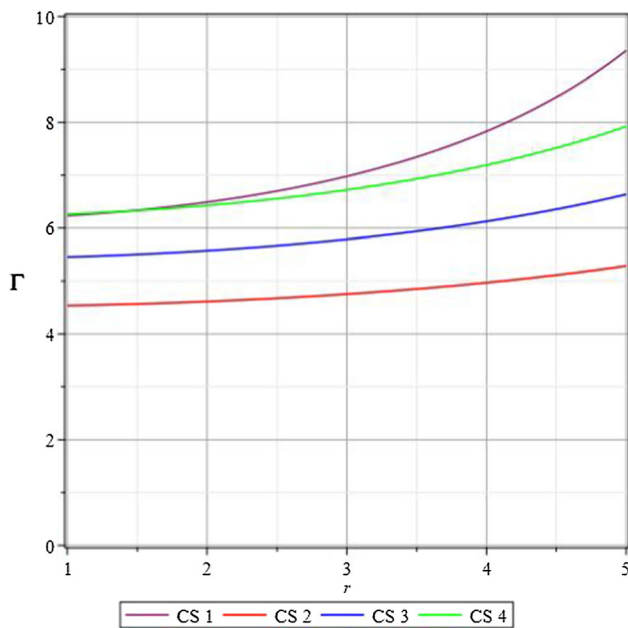


Fig. 8 Adiabatic index

compactness changes as one moves radially from the star’s center towards its surface. The compactification parameter, often signified by the limit of the redshift function $z_s < 4.77$, is a critical measure in understanding the stability and behavior of compact stars. This parameter is intimately linked to the redshift function z_s derived from the expression

$$z_s = \frac{1}{\sqrt{1 - \frac{2m(r)}{r}}} - 1. \tag{37}$$

The limit on z_s sets a crucial constraint on the compactness of the star. This boundary condition ensures the stability and viability of the compact object. Exceeding this limit may lead to gravitational collapse or other extreme phenomena that could destabilize the star’s structure.

Buchdahl’s proposal imposes a critical constraint on compact stars; the surface redshift must not exceed 5 to maintain stability [5]. Figure 12 confirms that the surface redshift z_s remains below this limit, validating the credibility of the anisotropic compact star model. This adherence to Buchdahl’s criterion reaffirms the model’s accuracy in representing the gravitational behavior of compact, self-gravitating objects.

$$m(r) = 4\pi \int_0^r r^2 \left(\frac{2R^2 \left(\left(a \left(Ar^2 - \frac{1}{2} \right) R^2 + 2r^2 b \left(Ar^2 - \frac{5}{4} \right) \right) R^2 e^{(-A+B)r^2+C} + \frac{R^2(aR^2+br^2)}{2} e^{Br^2+C} \right)}{\left(e^{Br^2+C} R^2 + (a-1) R^2 + br^2 \right) r^2 \left(aR^2 + br^2 \right)^2} + \frac{2R^2 \left((a-1) R^2 + br^2 \right) \left(\left(a \left(Ar^2 - \frac{1}{2} \right) R^2 + 2r^2 b \left(Ar^2 - \frac{5}{4} \right) \right) e^{-Ar^2} + \frac{ar^2}{2} + \frac{br^2}{2} \right)}{\left(e^{Br^2+C} R^2 + (a-1) R^2 + br^2 \right) r^2 \left(aR^2 + br^2 \right)^2} \right) dr. \tag{35}$$

Figure 10 portrays the monotonic nature of the mass function, showcasing its minimum value at the center of the stars. Additionally, the graph demonstrates that as r approaches 0, $m(r)$ tends towards 0, indicating the regularity of the mass function at the origin.

The behavior of the mass function also conveys insights into the compactness of the star. Compactness, often characterized by the ratio of mass to radius, provides a measure of how densely packed the stellar matter is. In the context of the mass function, the behavior of $m(r)$ near the origin signifies a regular distribution of mass, which is essential for a stable and well-defined compact object.

Compactness is defined as $u(r)$, and the compactness of a star at a given radius r is expressed as the ratio of the mass function, $m(r)$, to the radius r :

$$u(r) = \frac{m(r)}{r}. \tag{36}$$

The plot for $u(r)$ is generated using the expression for $m(r)$ obtained earlier, showcasing the variation of compactness across different radii within the star. Figure 11 illustrates this relationship, providing a visual representation of how the

4 Results and physical discussion of the model

In our investigation, we explored the construction of anisotropic compact stars within the Finslerian context, employing the Barthel connection. This significant approach treats each point in the Finsler manifold as a space point, simplifying the complex Finsler structure into a more manageable osculating Riemannian-like structure. Through this method, we derived equations that describe intricate Finslerian geometric properties in terms of simpler Christoffel symbols Γ^i_{jk} . Remarkably, these equations seamlessly transform into Riemannian structures as η approaches 1. This utilization of Finsler geometry offers a unique lens to discuss the dynamics of stellar objects, unveiling intriguing insights into their nature and behavior.

As mentioned earlier, the metric tensor’s configuration deviates from the conventional Riemannian geometry due to the presence of an anisotropic term. To complement this structure with the exterior Schwarzschild metric, a specific

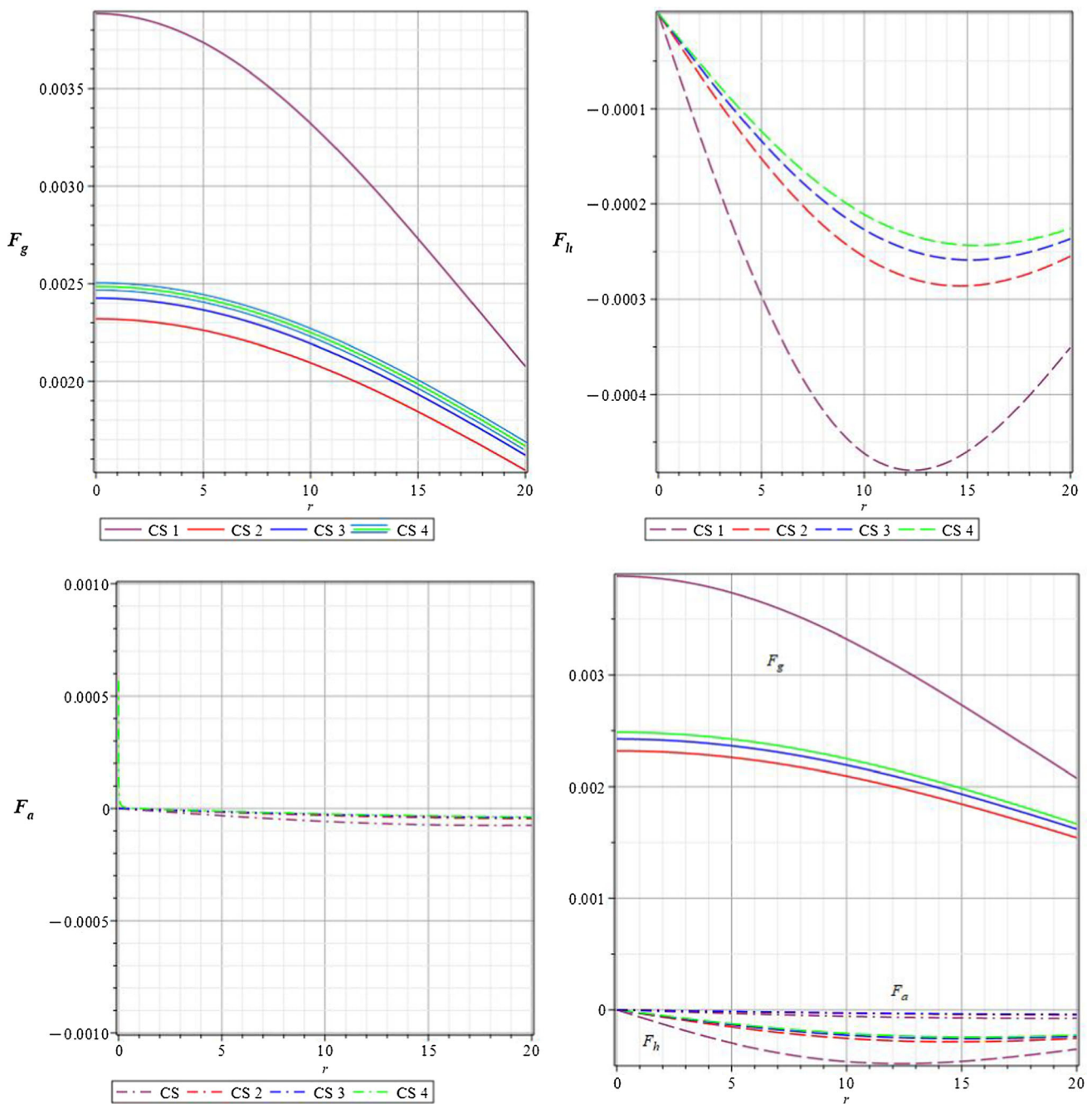


Fig. 9 Equilibrium conditions in anisotropic stars shaped by three forces

substitution for η was employed, elaborated in (15). This specific form unveils the anisotropic property of the space-time (universe), which helps to understand the low-scale anisotropy in the cosmic microwave background (CMB). In order to study such observation in a Finslerian background we plot the base structure through analysis of stellar objects in a Finslerian geometric background. In this regard, to evaluate the proposed model’s effectiveness, we explored four distinct compact stars, each accompanied by their respective

physical characteristics outlined in Table 1. Through strategic selections of metric potentials, we computed essential physical constants. Evaluating the model’s stability involved a thorough analysis of regularity conditions and the intrinsic physical properties embedded within the metric structure, detailed below.

1. Figures 1 and 2 offer visual representations of the metric potentials and the key matter variables ρ , p_r , p_t .

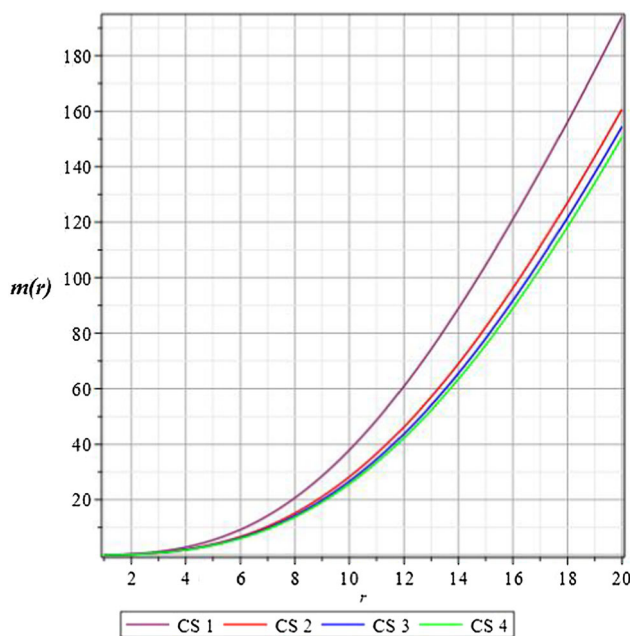


Fig. 10 Mass function ($m(r)$)

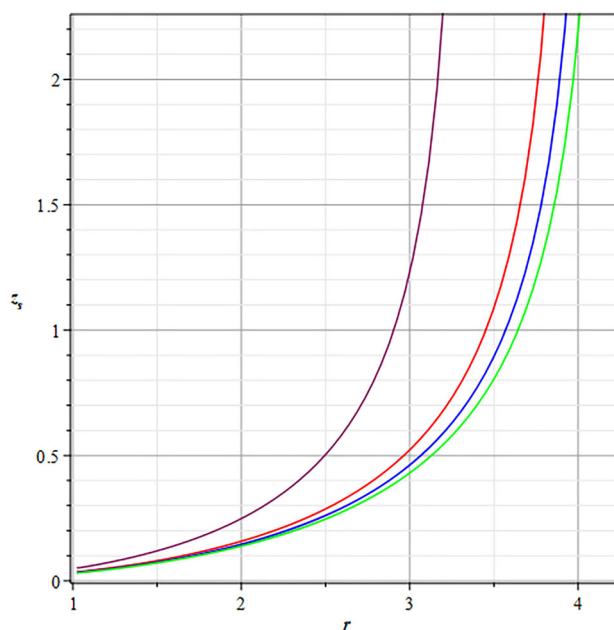


Fig. 12 Redshift parameter ($Z(r)$)

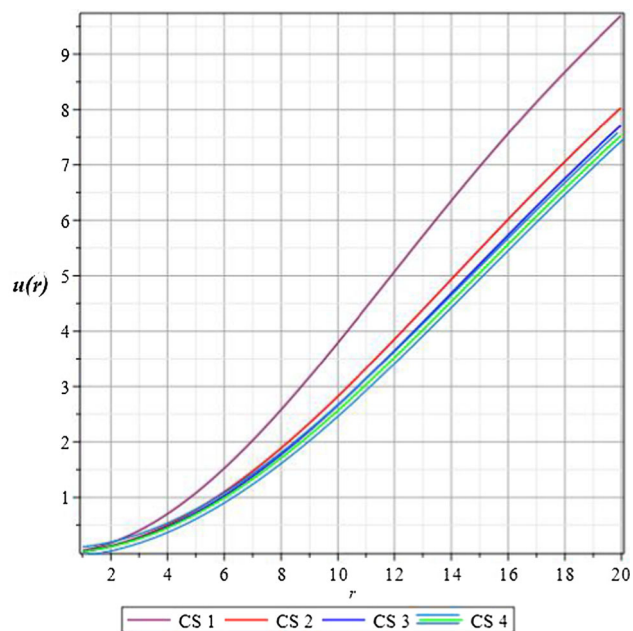


Fig. 11 Compactness parameter ($u(r)$)

These graphics effectively portray the declining trend observed in the distribution of matter, a vital characteristic expected within stellar configurations. Furthermore, our analysis of the radial derivative plots of matter densities unveils that derivatives gradually decrease and vanish at the center of the stars. This observation highlights an essential aspect of stellar composition, emphasizing the importance of the central regions within the overall structural integrity of the stars. The decrease in pressure

signifies the diminishing compressive forces acting on the star’s material layers. These physical details offer insights into the internal dynamics and stability of the proposed compact star model. The behavior of energy densities and pressures within the star elucidates the distribution of forces and material properties critical for the star’s equilibrium.

2. The investigation of energy conditions involved plotting graphs, depicted in Fig. 3, to assess the model’s adherence to these fundamental principles. The observed positive behavior not only confirms the satisfaction of energy conditions by the matter constituting the compact star but also highlights an essential aspect of physical stability. This compliance with energy conditions is pivotal, as it signifies the absence of negative energy densities or exotic matter, ensuring the physical stability of the compact star. By upholding these energy conditions, the model demonstrates a coherent and physically plausible structure, reinforcing its credibility as a stable and realistic representation of a compact stellar object.
3. In Fig. 4, the plot illustrating the anisotropic parameter showcases a smooth and consistent behavior spanning from the core to the outer boundaries of the stars. This force maintains stability, suggesting that compact stars rely on anisotropic forces to resist collapse, contributing to their structural integrity.
4. The model’s stability was examined, utilizing EoS parameters graphed in Fig. 5. This visualization not only highlights the EoS parameter’s consistent range within (0, 1), but also crucially addresses the physical stability aspect. The range of EoS parameters serves as a funda-

mental indicator of stability within physically acceptable boundaries. This adherence emphasizes the absence of negative energy densities or exotic matter, essential factors ensuring the physical stability of the compact star model.

5. Our investigation into the model's stability used Herrera's cracking condition, as in Figs. 6 and 7. The results indicate that $0 < v_{rs}^2, v_{st}^2 < 1$, and $|v_{st}^2 - v_{rs}^2| < 1$. These findings assure that the fluid within the stellar configuration remains stable, even after disturbances, suggesting resilience when external forces vanish from the system. This stability underscores the model's reliability in representing a stable compact stellar structure. A positive difference $v_{st}^2 - v_{rs}^2$ between sound velocities denotes stability. This condition ensures that perturbations propagate outwardly slower in the tangential direction compared to the radial direction, maintaining stability against collapse.
6. The adiabatic index, as depicted in Fig. 8, signifies the relationship between pressure and density variations within the star. It shows the star's ability to maintain stability despite compression or expansion without heat exchange with its surroundings. Physically, this stability implies that as the star's material compresses or expands, its internal energy remains constant, without significant alterations in its internal energy, contributing to the overall stability and resilience of the stellar structure.
7. The TOV equation (29) was adapted to FR background by leveraging the Riemannian equation and deriving expressions for three distinct forces F_g , F_h , and F_a . These force expressions were plotted in Fig. 9, revealing that the gravitational force precisely counterbalances the other two forces, ensuring stability within the compact star structure.
8. Figures 10, 11, and 12 depict the mass functions, compactness, and redshift, respectively. These plots exhibit a consistent increase with radius, reaching a maximum at the star's surface. The rising mass functions signify the accumulation of mass toward the star's outer layers, while increasing compactness indicates higher density towards the surface. Additionally, the ascending redshift values signify an intensified gravitational effect closer to the star's boundary. These trends collectively provide essential insights into the physical characteristics and dynamics governing the structure of the compact star.

Exploring anisotropic stars through the lens of Finslerian geometry unveils a unique perspective that transcends traditional differential geometry. This alternative geometric approach not only enhances our understanding of anisotropic stars but also opens pathways to contemplate various celestial bodies within the broader scope of Finsler geometry. The utilization of Finsler geometry to explore celestial bodies, par-

ticularly anisotropic stars, serves as a stepping stone towards broader applications and future research directions.

In future works we anticipate expanding this geometric approach to investigate a wider array of cosmic phenomena, such as neutron stars, black holes, or even the larger cosmic structures like galaxies and galaxy clusters. Exploring these diverse astronomical entities within the framework of Finsler geometry could unveil novel understandings of their formations, dynamics, and interactions. Moreover, researchers might delve deeper into the intricate interplay between Finsler geometry and fundamental physical theories, like general relativity or quantum mechanics. This exploration could lead to the development of more comprehensive and unified theories that integrate geometric concepts from Finslerian frameworks into the understanding of fundamental physical laws.

Acknowledgements Praveen J., S. K. Narasimhamurthy, and Yashwanth B. R. acknowledge the Department of Science and Technology (DST) in New Delhi, India, for providing research facility support through DST-FIST-2019. The authors express their sincere gratitude to the anonymous reviewer for their valuable suggestions which significantly improved the quality and presentation of the research. The first author thanks to University of Grant Commission, India, for supporting financially via UGC Junior Research Fellowship (student ID-231610191052)/(Dec-2022/June-2023-CSIR-UGC NET).

Author contributions Praveen J.: conceptualization, formal analysis, methodology, writing—original draft. S. K. Narasimhamurthy: visualization, supervision, project administration, investigation. Yashwanth B. R.: formal analysis, methodology, graphical analysis, script writing.

Funding No funding was received for this research.

Data Availability Statement Data will be made available on reasonable request.

Code Availability Statement The manuscript has no associated code/software. [Author's comment: No code is available.]

Declarations

Conflict of interest The authors confirm that there are no financial interests or personal affiliations that could have influenced the research presented in this paper.

Open Access This article is licensed under a Creative Commons Attribution 4.0 International License, which permits use, sharing, adaptation, distribution and reproduction in any medium or format, as long as you give appropriate credit to the original author(s) and the source, provide a link to the Creative Commons licence, and indicate if changes were made. The images or other third party material in this article are included in the article's Creative Commons licence, unless indicated otherwise in a credit line to the material. If material is not included in the article's Creative Commons licence and your intended use is not permitted by statutory regulation or exceeds the permitted use, you will need to obtain permission directly from the copyright holder. To view a copy of this licence, visit <http://creativecommons.org/licenses/by/4.0/>. Funded by SCOAP³.

Appendix

In our approach to study compact stars in the Finsler–Rander background, we utilize the osculating Riemannian method, and by employing the Barthel connection, we proceed as in [54, 55, 63, 64]. Let the nonvanishing vector field be denoted as $Y = B$, defined on M , where $B^i = a^{ij} B_j$. The global nonvanishing nature of the vector field B on M implies that β has nonzero points on M . This enables the application of the osculating Riemannian approach explore the structure of black holes within the context of Finsler geometry, emphasizing the necessity of a nonvanishing vector field for the black hole. Let b be the length of the vector field B with respect to α . Then, by the approach of osculation, we have

$$b^2 = a_{ij}(x) B^i B^j = B_i B^i = \alpha^2(x, y), \quad (\text{A1})$$

and for $\beta(x, y)$ 0 is expressed as a vector

$$\beta(x, y) = B_i y^i. \quad (\text{A2})$$

Here, $B_i = (\gamma(r), 0, 0, 0)$ is a vector with components $(\gamma(r), 0, 0, 0)$, and (y^i) represents the coordinates $(y^i) = (y^0, y^1, y^2, y^3) = (t, r, \theta, \phi)$. We incorporate the Barthel connection and consider that the 1-form $\beta(x, y)$ has a nonzero time component within compact stars. By this background using Eqs. (2)–(5) in Eq. (1), we derive the osculating FR metric (FR) metric as follows [54–56]:

$$\beta(x, B) = b^2 \quad \text{and} \quad Y_i(x, B) = B_i. \quad (\text{A3})$$

Then the B osculating Riemannian metric becomes

$$g_{ij} = \left(\frac{F}{\alpha} \right)_{y=B(x)} a_{ij}(x) + \left(\frac{1}{\alpha} (B_i y_j + B_j y_i) - \frac{\beta}{\alpha^3} y_i y_j + B_i B_j \right)_{y=B(x)}, \quad (\text{A4})$$

where $y_i = a_{ij} y^j$.

The Randers metric is a combination of the Riemannian metric tensor, denoted as $\alpha(x, y)$, and the 1-form $\beta(x, y)$, defined by $\alpha(x, y) = \sqrt{a_{ij}(x) y^i y^j}$ and $\beta(x, y) = b_i(x) y^i$. Thus,

$$F = \alpha(x, y) + \beta(x, y), \quad (\text{A5})$$

where $a_{ij}(x)$ represents the metric components of the Riemannian metric which is defined on the tangent space of each point of the manifold M , and $b_i(x)$ is the nonvanishing vector field. In this context, the Riemannian metric $\alpha(x, y)$ characterizes the isotropic and spherically symmetric nature of the universe's metric. The metric tensor (a_{ij}) of the Randers metric is expressed as follows:

$$a_{ij}(x) = \text{diag} \left(e^{\nu(r)}, -e^{\lambda(r)}, -r^2, -r^2 \sin^2 \theta \right). \quad (\text{A6})$$

Substituting above expressions (A3) and (A6) in Eq. (A4) it can be shown that the above complex metric structure (A4) reduces to a less complex structure,

$$g_{ij}(x) = (1 + \alpha) \left(a_{ij} + \frac{B_i B_j}{\alpha} \right). \quad (\text{A7})$$

Then the metric components are given by

$$g_{oo}(x) = (1 + \gamma(r)) (a_{00} + \gamma(r)), \quad (\text{A8})$$

$$g_{oj}(x) = (1 + \gamma(r)) \left(a_{00} + \frac{B_o B_j}{\alpha} \right), \quad (\text{A9})$$

$$g_{ij}(x) = (1 + \gamma(r)) a_{ij}, \quad \text{where, } ij \in \{1, 2, 3\}. \quad (\text{A10})$$

The resulting metric structure called an osculating Barthel–Finsler wormhole structure is given by

$$(g_{ij}(x)) = \text{diag} \left((\gamma + 1) (e^{\nu(r)} + \gamma), -(\gamma + 1) e^{\lambda(r)}, (\gamma + 1) r^2, -(\gamma + 1) r^2 \sin^2 \theta \right).$$

References

1. N.K. Glendenning, *Compact Stars: Nuclear Physics, Particle Physics and General Relativity* (Springer Science & Business Media, Berlin, 2012)
2. S.L. Shapiro, S.A. Teukolsky, *Black Holes, White Dwarfs, and Neutron Stars: The Physics of Compact Objects* (Wiley, New York, 2008)
3. R.C. Tolman, Static solutions of Einstein's field equations for spheres of fluid. *Phys. Rev.* **55**, 364 (1939)
4. J.R. Oppenheimer, H. Snyder, On continued gravitational contraction. *Phys. Rev.* **56**, 455 (1939)
5. K. Schwarzschild, On the gravitational field of a sphere of incompressible fluid according to Einstein's theory (1999). arXiv preprint [arXiv:physics/9912033](https://arxiv.org/abs/physics/9912033)
6. H.A. Buchdahl, General relativistic fluid spheres. *Phys. Rev.* **116.4**, 1027 (1959)
7. S. Chandrasekhar, Dynamical instability of gaseous masses approaching the Schwarzschild limit in general relativity. *Phys. Rev. Lett.* **12**(4), 114 (1964)
8. R.J. Adler, A fluid sphere in general relativity. *J. Math. Phys.* **15**(6), 727–729 (1974)
9. L. Herrera, Cracking of self-gravitating compact objects. *Phys. Lett. A* **165**(3), 206–210 (1992)
10. H. Abreu, H. Hernández, L.A. Núñez, Sound speeds, cracking and the stability of self-gravitating anisotropic compact objects. *Class. Quantum Gravity* **24.18**, 4631 (2007)
11. M.K. Gokhroo, A.L. Mehra, Anisotropic spheres with variable energy density in general relativity. *Gen. Relativ. Gravit.* **26**, 75–84 (1994)
12. H. Abreu, H. Hernández, L.A. Núñez, Sound speeds, cracking and the stability of self-gravitating anisotropic compact objects. *Class. Quantum Gravity* **24.18**, 4631 (2007)
13. S. Das et al., Modeling of compact stars: an anisotropic approach. *Gen. Relativ. Gravit.* **53**, 1–32 (2021)
14. S.K. Maurya, A. Banerjee, S. Hansraj, Role of pressure anisotropy on relativistic compact stars. *Phys. Rev. D* **97.4**, 044022 (2018)
15. M. Gleiser, K. Dev, Anisotropic stars: exact solutions and stability. *Int. J. Mod. Phys. D* **13**(07), 1389–1397 (2004)
16. B.V. Ivanov, Analytical study of anisotropic compact star models. *Eur. Phys. J. C* **77**, 1–12 (2017)

17. A. Errehymy, Y. Khedif, M. Daoud, Anisotropic compact stars via embedding approach in general relativity: new physical insights of stellar configurations. *Eur. Phys. J. C* **81**, 1–16 (2021)
18. S. Das et al., Modeling of compact stars: an anisotropic approach. *Gen. Relativ. Gravit.* **53**, 1–32 (2021)
19. S.K. Maurya et al., Anisotropic models for compact stars. *Eur. Phys. J. C* **75**(5), 225 (2015)
20. S.K. Maurya et al., Generalised model for anisotropic compact stars. *Eur. Phys. J. C* **76**, 1–12 (2016)
21. P. Bhar et al., Modelling of anisotropic compact stars of embedding class one. *Eur. Phys. J. A* **52.10**, 312 (2016)
22. M. Ilyas, Compact stars with variable cosmological constant in (R, T) gravity. *Astrophys. Space Sci.* **365**(11), 180 (2020)
23. M. Zubair, G. Abbas, I. Noureen, Possible formation of compact stars in $f(R, T)$ gravity. *Astrophys. Space Sci.* **361.1**, 8 (2016)
24. P. Saha, U. Debnath, Study of anisotropic compact stars with quintessence field and modified chaplygin gas in $f(T)$ gravity. *Eur. Phys. J. C* **79**, 1–16 (2019)
25. M.F. Shamir, S. Zia, Physical attributes of anisotropic compact stars in $f(R, G)$ gravity. *Eur. Phys. J. C* **77**, 1–12 (2017)
26. M. Jan et al., A structural analysis of self-gravitating anisotropic stars via equation of state in modified teleparallel gravity. *Results Phys.* 106662 (2023)
27. G.G.L. Nashed, S. Capozziello, Anisotropic compact stars in $f(R)$ gravity. *Eur. Phys. J. C* **81**(5), 481 (2021)
28. M. Sharif, M. Zeeshan Gul, Anisotropic compact stars with Karmarkar condition in energy-momentum squared gravity. *Gen. Relativ. Gravit.* **55.1**, 10 (2023)
29. A.K. Prasad et al., Relativistic model for anisotropic compact stars using Karmarkar condition. *Astrophys. Space Sci.* **364**, 1–12 (2019)
30. D.M. Pandya et al., Anisotropic compact star model satisfying Karmarkar conditions. *Astrophys. Space Sci.* **365**(2), 30 (2020)
31. P.L. Antonelli, R.S. Ingarden, M. Matsumoto, *The Theory of Sprays and Finsler Spaces with Applications in Physics and Biology*, vol. 58 (Springer Science & Business Media, Berlin, 1993)
32. B. David, S.-S. Chern, Z. Shen, *An Introduction to Riemann–Finsler Geometry*, vol. 200 (Springer Science & Business Media, Berlin, 2000)
33. H. Rund, *The Differential Geometry of Finsler Spaces*, vol. 101 (Springer Science & Business Media, Berlin, 2012)
34. R.S. Ingarden, M. Matsumoto, On the 1953 barthel connection of a finsler-space and its physical aspect. *Publ. Math. Debr.* **43**(1–2), 87–90 (1993)
35. R.S. Ingarden, L. Tamássy, The point Finsler spaces and their physical applications in electron optics and thermodynamics. *Math. Comput. Model.* **20**(4–5), 93–107 (1994)
36. M. Matsumoto, Theory of Y -extremal and minimal hypersurfaces in a Finsler space, on Wegener’s and Barthel’s theories. *J. Math. Kyoto Univ.* **26**(4), 647–665 (1986)
37. R.S. Ingarden, M. Matsumoto, On the 1953 Barthel connection of a Finsler space and its mathematical and physical interpretation. *Rep. Math. Phys.* **32**(1), 35–48 (1993)
38. M. Matsumoto, Theory of Finsler spaces with (α, β) -metric. *Rep. Math. Phys.* **31**(1), 43–83 (1992)
39. V.S. Sabau, H. Shimada, Classes of Finsler spaces with (α, β) -metrics. *Rep. Math. Phys.* **47.1**, 31–48 (2001)
40. L. Kozma, On osculation of Finsler-type connections. *Acta Math. Hung.* **53**(3–4), 389–397 (1989)
41. R.K. Tavakol, N. Van Den Bergh, Finsler spaces and the underlying geometry of space-time. *Phys. Lett. A* **112**(1–2), 23–25 (1985)
42. Yu. Bogoslovsky, A viable model of locally anisotropic space-time and the Finslerian generalization of the relativity theory. *Fortschr. Phys./Prog. Phys.* **42.2**, 143–193 (1994)
43. C. ShengLin, The theory of relativity on the Finsler spacetime. *J. Syst. Eng. Electron.* **6**(4), 239–252 (1995)
44. A.P. Kouretsis, M. Stathakopoulos, P.C. Stavrinou, General very special relativity in Finsler cosmology. *Phys. Rev. D* **79**(10), 104011 (2009)
45. C. Pfeifer, The Finsler spacetime framework. *Backgrounds for physics beyond metric geometry* (2013)
46. X. Li, Z. Chang, Exact solution of vacuum field equation in Finsler spacetime. *Phys. Rev. D* **90**(6), 064049 (2014)
47. P.C. Stavrinou, A.P. Kouretsis, FRW-metric and Friedmann equations in a generalized cosmological model. *J. Phys. Conf. Ser.* **68**(1) (2007)
48. Z. Chang, X. Li, Modified Friedmann model in Randers–Finsler space of approximate Berwald type as a possible alternative to dark energy hypothesis. *Phys. Lett. B* **676**(4–5), 173–176 (2009)
49. R. Raushan, R. Chaubey, Finsler–Randers cosmology in the framework of a particle creation mechanism: a dynamical systems perspective. *Eur. Phys. J. Plus* **135.2**, 228 (2020)
50. G. Papagiannopoulos et al., Dynamics in varying vacuum Finsler–Randers cosmology. *Eur. Phys. J. C* **80**, 1–22 (2020)
51. X. Li, S. Wang, Z. Chang, Anisotropic inflation in the Finsler spacetime. *Eur. Phys. J. C* **75**, 1–8 (2015)
52. Z. Nekouee et al., Finsler–Randers model for anisotropic constant-roll inflation. *Eur. Phys. J. Plus* **137**(12), 1388 (2022)
53. A. Triantafyllopoulos et al., Schwarzschild-like solutions in Finsler–Randers gravity. *Eur. Phys. J. C* **80**(12), 1200 (2020)
54. S.K. Narasimhamurthy, J. Praveen, Constant roll inflation and Finsler geometry: exploring anisotropic universe with scalar factor parametrization. *Eur. Phys. J. C* **84**(1), 60 (2024)
55. S.K. Narasimhamurthy, J. Praveen, Cosmological constant roll of inflation within Finsler–barthel–Kropina geometry: a geometric approach to early universe dynamics. *New Astron.* **108**, 102187 (2024)
56. J. Praveen, S.K. Narasimhamurthy, Exploring wormhole model in Finsler–Randers space-time (**Communicated**)
57. H.M. Manjunatha, S.K. Narasimhamurthy, The wormhole model with an exponential shape function in the Finslerian framework. *Chin. J. Phys.* **77**, 1561–1578 (2022)
58. K.P. Das, U. Debnath, Possible existence of traversable wormhole in Finsler–Randers geometry. *Eur. Phys. J. C* **83.9**, 821 (2023)
59. F. Rahaman et al., The Finslerian wormhole models. *Eur. Phys. J. C* **76**, 1–9 (2016)
60. F. Rahaman et al., The Finslerian compact star model. *Eur. Phys. J. C* **75**, 1–12 (2015)
61. S.R. Chowdhury et al., Charged anisotropic strange stars in Finslerian geometry. *Eur. Phys. J. C* **79**, 1–15 (2019)
62. S.R. Chowdhury et al., Anisotropic strange star inspired by Finsler geometry. *Int. J. Mod. Phys. D* **29.01**, 2050001 (2020)
63. R. Hama et al., Cosmological evolution and dark energy in osculating Barthel–Randers geometry. *Eur. Phys. J. C* **81.8**, 742 (2021)
64. R. Hama, T. Harko, S.V. Sabau, Dark energy and accelerating cosmological evolution from osculating Barthel–Kropina geometry. *Eur. Phys. J. C* **82**(4), 385 (2022)